

$O(\alpha_s^3)$ analysis of inclusive jet and di-jet production in heavy ion reactions at the Large Hadron Collider

Yuncun He^a, Ivan Vitev^b, Ben-Wei Zhang^a

^aKey Laboratory of Quark and Lepton Physics (Central China Normal University), Ministry of Education, China

^bLos Alamos National Laboratory, Theoretical Division, MS B238, Los Alamos, NM 87545, U.S.A.

Abstract

Jets physics in heavy ion reactions is an important new area of active research at the Relativistic Heavy Ion Collider (RHIC) and at the Large Hadron Collider (LHC) that paves the way for novel tests of QCD multi-parton dynamics in dense nuclear matter. At present, perturbative QCD calculations of hard probes in elementary nucleon-nucleon reactions can be consistently combined with the effects of the nuclear medium up to $O(\alpha_s^3)$. While such accuracy is desirable but not necessary for leading particle tomography, it is absolutely essential for the new jet observables. With this motivation, we present first results and predictions to $O(\alpha_s^3)$ for the recent LHC lead-lead (Pb+Pb) run at a center-of-mass energy of 2.76 TeV per nucleon-nucleon pair. Specifically, we focus on the suppression of the single and double inclusive jet cross sections. Our analysis includes not only final-state inelastic parton interactions in the QGP, but also initial-state cold nuclear matter effects and an estimate of the non-perturbative hadronization corrections. We demonstrate how an enhanced di-jet asymmetry in central Pb+Pb reactions at the LHC, recently measured by the ATLAS and CMS experiments, can be derived from these results. We show quantitatively that a fraction of this enhancement may be related to the ambiguity in the separation between the jet and the soft background medium and/or the diffusion of the parton shower energy away from the jet axis through collisional processes. We point to a suite of measurements that can help build a consistent picture of parton shower modification in heavy ion collisions at the LHC.

1. Introduction

One of the most intensively studied processes in high-energy physics is jet production, which can be used to accurately test the fundamental properties of Quantum Chromodynamics (QCD) and explore new physics beyond the Standard Model [1]. At the parton level, jet observables, such as cross sections, jet shapes or event shapes, can be computed systematically and reliably order-by-order in perturbative Quantum Chromodynamics (pQCD). At the hadron level, non-perturbative effects related to hadronization and the underlying event can be estimated and combined with the pQCD results to produce theoretical prediction suitable for comparison to the experimental measurements [1, 2, 3, 4]. The highest center-of-mass energy hadronic collisions available to date at the CERN Large Hadron Collider (LHC) guarantee an abundant yield of large transverse momentum hadrons and jets and provide, through experimental measurements and constraints on theoretical models [5, 6], an ideal opportunity to advance perturbative QCD.

In relativistic heavy ion collisions at the LHC, jet and particle production will be altered by the collisional and radiative final-state interactions of the parent partons which propagate through a region of hot and dense deconfined matter, or the

quark-gluon plasma (QGP). It has been demonstrated that a significant part of the partons' energy can be lost due to medium-induced gluon bremsstrahlung [7], and uncertainties in energy loss calculations have been commented upon in [8]. The predicted related suppression of leading particles at the Relativistic Heavy Ion Collider (RHIC) and at the LHC [9] is now well established [10, 11, 12], including its non-trivial momentum dependence verified by the ALICE Collaboration. On the other hand, the modification of jets in dense QCD matter requires much deeper understanding of the in-medium parton shower production mechanisms [13]. For inclusive jets, tree-level calculations can be used to discuss qualitatively the effects of final-state interactions but $O(\alpha_s^3)$ results [14] are necessary for quantitative comparison to the preliminary jet experimental data in gold-gold (Au+Au) and copper-copper (Cu+Cu) reactions at RHIC [15, 16, 17]. For tagged jets and di-jets lowest order, for example $O(\alpha_s^2)$, $O(G_F\alpha_s)$ and $O(\alpha_{em}\alpha_s)$, calculations fail to describe even qualitatively the double differential momentum distributions [18] and one-loop pQCD results are required.

Recently the ATLAS and CMS Collaborations reported a significant enhancement in the transverse momentum imbalance of di-jets produced in central Pb+Pb collisions at the LHC [19, 20]. It has been qualitatively argued that such asymmetry A_J may be a consequence of jet quenching in the QGP created in heavy ion reactions at LHC [21]. Attempts to explain its magnitude based on Monte Carlo simulations with a Pythia generated p+p baseline have also been presented [22, 23, 24]. In Ref. [25] the important observation was made that the huge

Email addresses: heyc@iopp.ccnu.edu.cn (Yuncun He^a), ivitev@lanl.gov (Ivan Vitev^b), bwzhang@iopp.ccnu.edu.cn (Ben-Wei Zhang^a)

heavy ion background and its fluctuations may significantly enhance the di-jet asymmetry distribution.

In this Letter we report first results and predictions at $O(\alpha_s^3)$ for inclusive jet and di-jet productions in central Pb+Pb collisions with $\sqrt{s_{NN}} = 2.76$ TeV at the LHC. We combine consistently the $O(\alpha_s^3)$ calculations in nucleon-nucleon reactions, validated through comparison to the $\sqrt{s} = 7$ TeV p+p data at the LHC, with parton energy loss effect in the hot QCD medium at $O(\alpha_s^2 \alpha_s^{\text{rad}})$ [26]. $O(\alpha_s^3)$, $O(\alpha_s^2 \alpha_s^{\text{rad}})$ results represent next-to-leading order accuracy for inclusive jet production but for the more differential observables, such as the di-jet asymmetry at $A_J > 0$, this may be the first order that gives a non-trivial ($\neq 0$) contribution. We demonstrate the relation between the cross section attenuation for inclusive jets and di-jets and the resulting enhancement in the di-jet asymmetry A_J . We find that a part of this enhancement may arise from the uncertainty in the jet/background separation and/or the dissipation of the energy from the shower into the QGP due to collisional processes [27]. To further differentiate these two possibilities is subject of future work.

Our Letter is organized as follows: we present benchmark results for inclusive jet and di-jet production in $\sqrt{s} = 7$ TeV p+p collisions at the LHC in section 2. Results and predictions for the central Pb+Pb reactions at the LHC at $\sqrt{s_{NN}} = 2.76$ TeV are given in section 3. Our conclusions are presented in section 4.

2. Inclusive jet and di-jet production in p+p collisions

Within the framework of the collinear perturbative QCD factorization approach the lowest order (LO) single and double inclusive jet production cross sections can be obtained from:

$$\frac{d\sigma}{dy_1 dy_2 d^2 E_{T1} d^2 E_{T2}} = \sum_{ab,ij} \frac{\delta(\Delta\varphi_{1,2} - \pi) \delta(E_{T1} - E_{T2})}{E_{T2}} \times \frac{\phi_{a/N}(x_a) \phi_{b/N}(x_b)}{x_a x_b} \frac{\alpha_s^2}{s^2} |\overline{M}_{ab \rightarrow ij}|^2. \quad (1)$$

In Eq. (1) $s = (P_a + P_b)^2$ is the squared center-of-mass energy of the hadronic collision and $d^2 E_T = E_T dE_T d\varphi$ with φ being the azimuthal angle of the jet.

$$x_a = \frac{p_a^+}{P_a^+} = \frac{E_{T1}}{\sqrt{s}} (e^{y_1} + e^{y_2}), \quad x_b = \frac{p_b^-}{P_b^-} = \frac{E_{T2}}{\sqrt{s}} (e^{-y_1} + e^{-y_2})$$

are the lightcone momentum fractions of the incoming partons. We denote by $\phi_{a,b/N}(x_{a,b})$ the distribution function of partons a, b in the nucleon. $|\overline{M}_{ab \rightarrow ij}|^2$ are the squared matrix elements for $a + b \rightarrow i + j$ processes, for massless partons see [28]. In the double collinear approximation the jets are produced back-to-back and identified with the parent partons. Formally, the partonic cross section in Eq. (1) is convolved with the jet phase space $S_2(p_1^\mu, p_2^\mu)$ (dimensionless in our convention). At tree level, this phase space factor is simply a sum of products of δ -functions. For inclusive jet production, the second jet is integrated out.

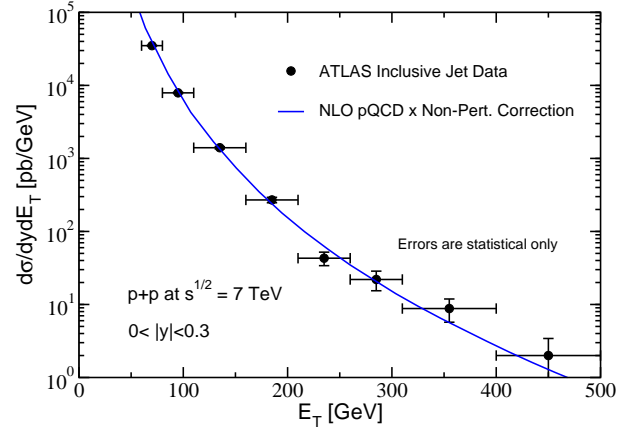


Figure 1: Comparison between the $R = 0.4$ inclusive jet cross section measured by the ATLAS Collaboration in p+p collisions at $\sqrt{s} = 7$ TeV and the $O(\alpha_s^3)$ QCD theory which includes non-perturbative corrections. Experimental error bars are statistical only.

The first obvious deficiency of the LO formalism is its inability to describe the jet radius dependence of the physical observables [14]. The second much more significant shortcoming is the inadequate description of the differential distribution of tagged jets [18] and di-jets due to the δ -function constraint in Eq. (1). At $O(\alpha_s^3)$ and beyond jets are defined by the jet-finding algorithms characterized by a radius parameter $R = \sqrt{\Delta y^2 + \Delta \phi^2}$, which gives the jet's spacial extent in rapidity y and azimuthal angle ϕ . Generally, the cross sections of the jet production at the $O(\alpha_s^3)$ can be expressed as [29]:

$$\frac{d\sigma}{dV_n} = \frac{1}{2!} \int dV_2 \frac{d\sigma(2 \rightarrow 2)}{dy_1 dy_2 d^2 E_{T1} d^2 E_{T2}} S_2(p_1^\mu, p_2^\mu) + \frac{1}{3!} \int dV_3 \frac{d\sigma(2 \rightarrow 3)}{dy_1 dy_2 dy_3 d^2 E_{T1} d^2 E_{T2} d^2 E_{T3}} \times S_3(p_1^\mu, p_2^\mu, p_3^\mu), \quad (2)$$

where $V_n = dy_1 \cdots dy_n d^2 E_{T1} \cdots d^2 E_{Tn}$ represents the phase space for multi-jets or multi-partons, respectively. The first term on the right-hand side of Eq. (2) gives the contribution from $2 \rightarrow 2$ processes, including the $O(\alpha_s^3)$ virtual corrections. The second term in Eq. (2) denotes the contribution from $2 \rightarrow 3$ processes. The jet size R and algorithm dependence are contained in the function $S_3(p_1^\mu, p_2^\mu, p_3^\mu)$ [14], which is significantly more complicated than $S_2(p_1^\mu, p_2^\mu)$. In the calculations that follow we will take advantage of the Ellis, Kunszt and Soper (EKS) numerical implementation of $O(\alpha_s^3)$ jets production in hadron-hadron collisions [29] and the CTEQ6.1M parametrization set of parton distribution functions [39].

Measurements of inclusive jet production in p+p collisions at $\sqrt{s} = 7$ TeV with jet cone radii $R = 0.4, 0.6$ and in different rapidity regions have been carried out by the ATLAS Collaboration at the LHC [5]. Perturbative QCD calculations can be corrected to the hadron level using parametrization of universal non-perturbative effects $f_{NP}(E_T, R)$ extracted from Monte Carlo

simulations as follows:

$$\frac{d\sigma^{\text{hadron}}}{dE_{T1} \cdots dE_{Tn}} = \frac{d\sigma^{\text{parton}}}{dE_{T1} \cdots dE_{Tn}} \prod_{i=1}^n f_{\text{NP}}(E_{Ti}, R_i). \quad (3)$$

In this Letter we employ the parametrization of non-perturbative effects provided by ATLAS [5] in all calculations except the ones presented in the bottom panel of Fig. 6. The only observables that are noticeably affected by f_{NP} are the ones that involve too significantly different radii R_1, R_2 . Returning to jet production in p+p collisions, we find that an excellent description of the differential jet spectrum is obtained in the measured region of E_T between 50 GeV and 500 GeV where the yield falls by more than 5 orders of magnitude. We present one example for rapidity $|y| < 0.3$ and $R = 0.4$ in Fig. 1. Variation of the factorization and renormalization scale $\mu_f = \mu_R = E_T$ in the interval $(E_T/2, 2E_T)$ has less than 10% effect on the inclusive jet cross section.

The evaluation of di-jet production in hadronic reactions is slightly more involved. At $O(\alpha_s^3)$ the naive exact transverse energy equality $E_{T1} = E_{T2}$ between the two jets is broken by $2 \rightarrow 3$ parton splitting processes. Loop corrections in $2 \rightarrow 2$ processes, proper jets definitions and finite E_T bins ensure well-behaved physical cross sections. To quantify the resulting imbalance we modify the $O(\alpha_s^3)$ EKS code [29] and define the dimensionless:

$$\tilde{\sigma} = \left[\frac{1}{nb} \right] E_{T1} E_{T2} \frac{d\sigma}{dE_{T1} dE_{T2}} \quad (4)$$

for brevity. In Fig. 2 we show the three-dimensional (3D) plot of $\tilde{\sigma}$ as a function of the transverse energy of the two jets E_{T1} and E_{T2} in the rapidity region $|y| < 2.8$ for the same jet size $R = 0.4$. Transverse energy bins $\Delta E_{T1}, \Delta E_{T2} = 10$ GeV have been chosen. While the cross section reaches its maximum for $E_{T1} \approx E_{T2}$, its most striking feature is how broad and slowly varying the di-jet yield is away from the main diagonal. As we will see below, such broad distribution limits the additional asymmetry that jet propagation in the QGP will induce.

One particular distribution that can be extracted from our general di-jet cross section calculation is that of the di-jet asymmetry A_J , defined as

$$A_J = \frac{E_{T1} - E_{T2}}{E_{T1} + E_{T2}}. \quad (5)$$

Making a change of variables from (E_{T1}, E_{T2}) to (A_J, E_{T2}) with $E_{T1} = E_{T2}(1+A_J)/(1-A_J)$ and then integrating over y_1, y_2, E_{T2} we can express the A_J distribution from the di-jet E_{T1}, E_{T2} spectrum as follows:

$$\begin{aligned} \frac{d\sigma}{dA_J} &= \int_{y_1 \min}^{y_1 \max} dy_1 \int_{y_2 \min}^{y_2 \max} dy_2 \int_{E_{T2} \min}^{E_{T2} \max} dE_{T2} \\ &\frac{2E_{T2}}{(1-A_J)^2} \frac{d\sigma[E_{T1}(A_J, E_{T2})]}{dy_1 dy_2 dE_{T1} dE_{T2}}, \end{aligned} \quad (6)$$

where $E_{T2 \max}$ is given by the jet production kinematics. By evaluating $A_J > 0$ we ensure that $E_{T1} > E_{T2}$. Note that at LO we always have $A_J = 0$.

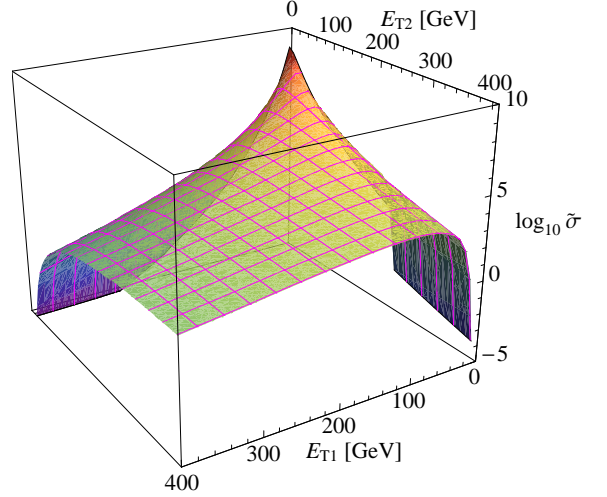


Figure 2: A three-dimensional representation of the $O(\alpha_s^3)$ di-jet cross section $\tilde{\sigma}$, defined in Eq. (4), in $\sqrt{s} = 7$ TeV p+p collisions at the LHC versus E_{T1} and E_{T2} . We have used a jet radius $R = 0.4$ and a rapidity interval $|y| < 2.8$.

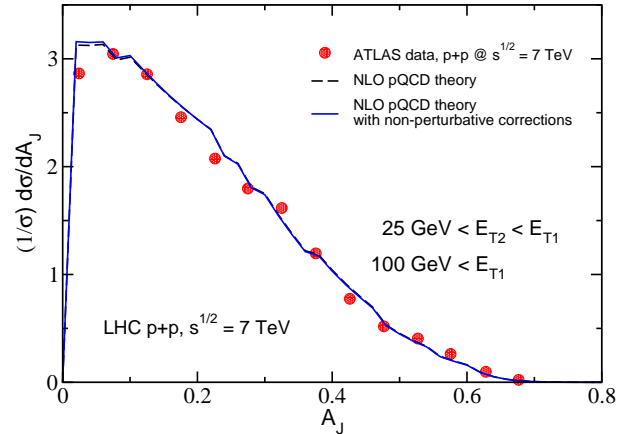


Figure 3: The normalized differential distribution of the di-jet asymmetry A_J , defined in Eq. (5), is evaluated at $O(\alpha_s^3)$ and compared to the ATLAS experimental measurement at $\sqrt{s} = 7$ TeV. Solid (dashed) lines include (do not include) non-perturbative corrections, respectively.

With the $O(\alpha_s^3)$ numerical results for $\tilde{\sigma}$ at hand, we can easily compute $\sigma^{-1} d\sigma/dA_J$ from Eq. (6) and confront it with the experimental data. The ATLAS Collaboration has measured the di-jet asymmetry distribution in p+p reactions at $\sqrt{s} = 7$ TeV with the following kinematics cuts: $E_{T1} > 100$ GeV for the leading jet and $E_{T2} > 25$ GeV for the subleading jet [19]. The corresponding comparison to the perturbative QCD theory is presented in Fig. 3 and shows excellent agreement. Variation of the factorization and renormalization scale $\mu_f = \mu_R = E_T$ in the interval $(E_T/2, 2E_T)$ has less than 2% effect on the A_J distribution. The dashed line represents the parton level $O(\alpha_s^3)$ results and the solid line includes non-perturbative effects, which are seen to be practically negligible for this observable. Strict transverse energy ordering $E_{T2} < E_{T1}$ for the leading and subleading jets implies $d\sigma/dA_J = 0$ when $A_J = 0$.

Fixed $O(\alpha_s^3)$ calculations of $d\sigma/dA_J$ will diverge for $A_J \rightarrow 0$. To ensure proper cancellation of real and virtual contributions to the physical cross section, these evaluations rely on finite bin sizes in transverse energy, rapidity and azimuth. For example, in numerical simulations based on the EKS code, results are calculated at random positions in phase space and any required grid for the differential cross sections is given by interpolation with a Gaussian smearing function [29]. Thus, our numerical simulations yield continuously smooth results of $E_{T1} \approx E_{T2}$ or, equivalently, $A_J \approx 0$. On the other hand, fine resolution cannot be achieved when $E_{T1} \rightarrow E_{T2}$ or $A_J \rightarrow 0$. To investigate this region, resummation beyond fixed order calculations will be needed.¹

3. Inclusive jet and di-jet production in heavy ion collisions

The bases for the evaluation of multi-jet cross sections in heavy ion collisions are the corresponding cross sections in the more elementary nucleon-nucleon reactions. In Ref. [30] it was shown that in QCD the final-state process-dependent medium-induced radiative corrections factorize in the production cross sections for the example of a single jet. The generalization to multiple jets proceeds as follows

$$d\sigma(\epsilon_1, \dots, \epsilon_n)_{\text{quench.}}^{n\text{-jet}} = d\sigma(\epsilon_1, \dots, \epsilon_n)_{\text{pp}}^{n\text{-jet}} \otimes P_1(\epsilon_1) \dots \otimes P_n(\epsilon_n) |J_1(\epsilon_1)| \dots |J_n(\epsilon_n)|. \quad (7)$$

Here, $P_i(\epsilon_i)$ is the probability that the i th jet will lose a fraction ϵ_i of its energy, $|J_i(\epsilon_i)|$ are phase space Jacobians, and \otimes denotes an integral convolution. Any dependence on the jet reconstruction parameters is not shown explicitly in Eq. (7). Furthermore, possible small contributions of the medium-induced parton shower associated with one jet to other jets that are very close in phase space (y, ϕ) are not included. For inclusive and approximately back-to-back jets that we consider in this Letter, this effect is negligible.

The application of Eq. (7) to inclusive jet production has been discussed extensively in Refs. [13, 14], where the angular distribution of the medium-induced gluon radiation is computed using the Reaction operator approach [7, 35]. Here, we summarize the main result. The medium-modified jet cross section per binary scattering is evaluated as

$$\frac{1}{\langle N_{\text{bin}} \rangle} \frac{d\sigma^{\text{AA}}(R)}{dy_1 dE_{T1}} = \sum_{q,g} \int_{\epsilon_1=0}^1 d\epsilon_1 P_{q,g}(\epsilon_1, E_{T1}) \times \frac{1}{(1 - [1 - f(R_1, p_{T1}^{\min})_{q,g}] \epsilon_1)} \frac{d\sigma_{q,g}^{\text{CNM,NLO}}(E'_{T1})}{dy_1 dE'_{T1}}. \quad (8)$$

In Eq. (8) the phase space Jacobian reads

$$|J_i(\epsilon_i)| = 1 / (1 - [1 - f(R_i, p_{Ti}^{\min})_{q,g}] \epsilon_i),$$

and $E'_{Ti} = |J_i(\epsilon_i)| E_{Ti}$ in the argument of $\sigma_{q,g}^{\text{CNM,NLO}}$. Note that in the expression above we have denoted by

$$f(R_i, p_{Ti}^{\min})_{q,g} = \frac{\int_0^{R_i} dr \int_{p_{Ti}^{\min}}^{E_{Ti}} d\omega \frac{dI_{q,g}^{\text{rad}}(i)}{d\omega dr}}{\int_0^{R_i} dr \int_0^{E_{Ti}} d\omega \frac{dI_{q,g}^{\text{rad}}(i)}{d\omega dr}}, \quad (9)$$

the part of the fractional energy loss ϵ_i that is redistributed inside the jet. Thus, $f(R_i, p_{Ti}^{\min})_{q,g}$ plays a critical role in defining the contribution (or lack thereof if $f(R_i, p_{Ti}^{\min})_{q,g} \rightarrow 0$) of the medium-induced bremsstrahlung to the jet. Note that in Eq. (9) p_{Ti}^{\min} is a parameter that can be used to simulate processes that can alter the energy of the jet beyond medium-induced bremsstrahlung. For example, by choosing $p_{Ti}^{\min} > 0$ GeV one can investigate phenomenologically the uncertainty in the jet/background separation and the diffusion of the parton shower energy away from the jet axis due to collisional processes. Specifically, one can adjust the value of p_{Ti}^{\min} to reflect the collisional energy loss of the parton shower $\langle \delta E_T \rangle$ evaluated in Ref. [27].

Cold nuclear matter (CNM) effects prior to the QGP formation, such as initial-state energy loss, coherent power corrections and the Cronin effect [31], can be incorporated in the cross sections for quark and gluon jet production $\frac{d\sigma_{q,g}^{\text{CNM,NLO}}}{dy dE_T}$ and their multi-jet generalization. At the LHC we are interested in jets of $E_T > 20$ GeV and at these energy scales of the effects listed above only initial-state energy loss, which is also derived in the framework of the Reaction operator approach, may play a role [32, 33]. In this work we evaluate the effects of cold nuclear matter on jet production in Pb+Pb collisions at the LHC and comment on their relevance to specific observables.

For di-jets produced in heavy ion reactions, the corresponding cross section can be expressed as

$$\frac{1}{\langle N_{\text{bin}} \rangle} \frac{d\sigma^{\text{AA}}(R)}{dy_1 dy_2 dE_{T1} dE_{T2}} = \sum_{qq, qg, gg} \int_{\epsilon_1=0}^1 d\epsilon_1 \int_{\epsilon_2=0}^1 d\epsilon_2 \frac{P_{q,g}(\epsilon_1, E_{T1})}{(1 - [1 - f(R_1, p_{T1}^{\min})_{q,g}] \epsilon_1)} \frac{P_{q,g}(\epsilon_2, E_{T2})}{(1 - [1 - f(R_2, p_{T2}^{\min})_{q,g}] \epsilon_2)} \times \frac{d\sigma_{qq, qg, gg}^{\text{CNM,NLO}}(E'_{T1}, E'_{T2})}{dy_1 dy_2 dE'_{T1} dE'_{T2}}. \quad (10)$$

The evaluation of the inclusive and di-jet cross sections at the LHC proceeds as follows: the hard jet production processes are distributed in the transverse plane according to the binary collision density $\sigma_{\text{in}}(dT_{AA}(b)/d\mathbf{x}_{\perp})$. The density of the QGP is taken to be proportional to the participant density $dN_{\text{part.}}/d\mathbf{x}_{\perp}$. Through isospin symmetry, necessary to account for the neutral particles, and parton-hadron duality [13] the gluon rapidity density in central Pb+Pb collisions at the LHC at $\sqrt{s_{NN}} = 2.76$ TeV is estimated to be $dN^g/dy = 2650$ from the ALICE experimental measurement of $dN^{\text{ch}}/d\eta$ [34]. We take into account the longitudinal Bjorken expansion of the medium and, by assuming local thermal equilibrium, we can evaluate the physical quantities, such as the Debye screening scale, the in-medium jet scattering cross sections, and the mean free paths [13, 14], that are employed in the calculation of the radiative energy loss [32].

¹We thank the reviewer for a suggestion to clarify this point.

The energy loss calculation, which uses the collision geometry described above, includes kinematic constraints, and provides the fully differential distribution of the medium-induced bremsstrahlung [32], is computationally demanding and performed separately. Using the analytic leading power dependence (up to logarithmic corrections) of the energy loss on the coupling between the jet and the medium g_{med} and the path of the parton propagation in the QGP:

$$\frac{dN^g}{d\omega d^2\mathbf{k}_\perp} \sim g_{\text{med}}^4 \int_0^\infty t \rho(\mathbf{x}_{0\perp} + \mathbf{n}_\perp t, t) dt, \quad (11)$$

we can precisely account for/study the sensitivity to the details of the in-medium jet dynamics by scaling the averaged bremsstrahlung spectra. Note that $g_{\text{med}}^2/4\pi$ above should not be confused with α_s^{rad} in the medium-induced bremsstrahlung vertex. In Eq. (11) $\mathbf{x}_{0\perp}$ is the jet or di-jet production point in the transverse plane and \mathbf{n}_\perp is the direction of its propagation. Finally, we evaluate in real time the probability distribution for the parent partons to lose fractions of their energy $\epsilon_i = \sum_n (\omega_n)_i / E_i$ due to multiple gluon emissions in the Poisson approximation [9]:

$$\int_0^1 P_{q,g}(\epsilon_i) d\epsilon_i = 1, \quad \int_0^1 \epsilon_i P_{q,g}(\epsilon_i) d\epsilon_i = \left\langle \frac{\Delta E_i}{E_i} \right\rangle_{q,g}. \quad (12)$$

This approximation is consistent with the inclusive gluon emission calculations currently used in jet quenching phenomenology [7, 35].

3.1. Quenching of inclusive jets

To investigate jet production in relativistic heavy ion collisions and quantify its deviation from the baseline results in elementary hadron-hadron reactions we define a generalized nuclear modification factor for multi-jet final states as follows:

$$R_{AA}^{\text{n-jet}}(E_{T1} \cdots E_{Tn}; R_1 \cdots R_n, p_{T1}^{\text{min}} \cdots p_{Tn}^{\text{min}}) = \frac{\frac{d\sigma^{AA}(E_{T1} \cdots E_{Tn}; R_1 \cdots R_n, p_{T1}^{\text{min}} \cdots p_{Tn}^{\text{min}})}{dy_1 \cdots dy_n dE_{T1} \cdots dE_{Tn}}}{\langle N_{\text{bin}} \rangle \frac{d\sigma^{pp}(E_{T1} \cdots E_{Tn}; R_1 \cdots R_n, p_{T1}^{\text{min}} \cdots p_{Tn}^{\text{min}})}{dy_1 \cdots dy_n dE_{T1} \cdots dE_{Tn}}}. \quad (13)$$

Next, we calculate numerically the cross sections and nuclear modification factors $R_{AA}^{\text{n-jet}}$ for inclusive jet and di-jet production ($n = 1, 2$) in central Pb+Pb collisions at LHC with $\sqrt{s_{NN}} = 2.76$ TeV.

Fig. 4 illustrates the dependence of the suppression ratio $R_{AA}^{1\text{-jet}}$ for inclusive jets in central Pb+Pb collisions on the jet size R . The top panel shows the net suppression resulting from both initial-state and final-state effects for $R = 0.2, 0.6$ and the bands represent the variation in coupling strength between the jet and the medium. The dashed, solid, and dot-dashed lines correspond to $g_{\text{med}} = 1.8, 2, 2.2$, respectively. Note that for small radii the suppression of jets can be comparable in magnitude to the suppression of inclusive particles. This is illustrated by including a reference charged hadron quenching measurement by the ALICE Collaboration [12] in Fig. 4. Preliminary

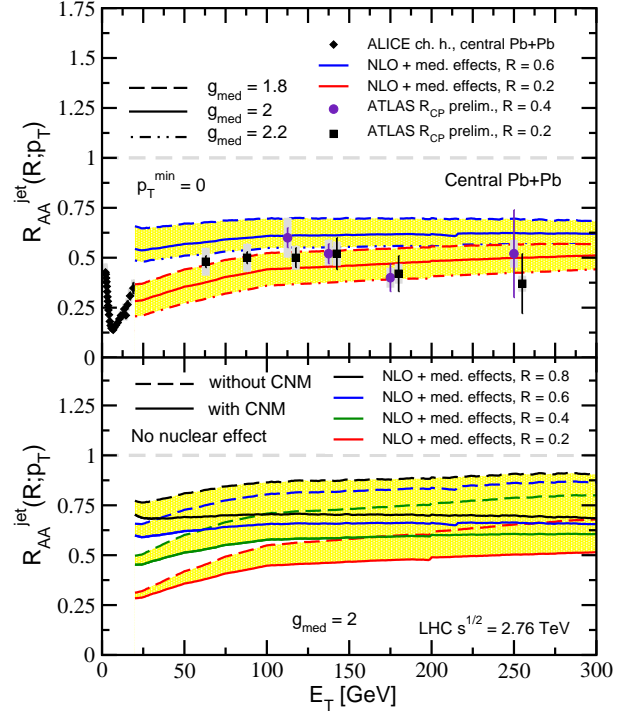


Figure 4: Top panel: the E_T dependence of the nuclear modification factor for different jet cone sizes $R = 0, 2, 0.6$ is calculated in central Pb+Pb collisions at the LHC $\sqrt{s_{NN}} = 2.76$ TeV. Bands represent the variation in the coupling strength between the jet and the medium. Bottom panel: the relative contribution of cold nuclear matter effects to R_{AA} is illustrated for $R = 0.2, 0.4, 0.6, 0.8$. ALICE experimental data on charged hadron suppression in central Pb+Pb collision is shown for reference. Preliminary ATLAS R_{CP} data is also shown for both $R = 0.2, 0.4$.

ATLAS data [36] on $R_{CP}^{1\text{-jet}}$, a ratio similar to $R_{AA}^{1\text{-jet}}$ where peripheral A+A reactions are used as a baseline, has now been included in the figure². The bottom panel of Fig. 4 presents a calculation for $R = 0.2, 0.4, 0.6, 0.8$ and for a fixed $g_{\text{med}} = 2$ with (solid line) or without (dashed line) cold nuclear matter effects. For fixed centrality, CNM effects, here dominated by initial-state energy loss, do not depend on the jet size or jet finding algorithm and become more relevant, relatively speaking, for large radii R . Even though on an absolute scale this additional suppression is not very large, it is more significant in comparison to the Z^0 or Dell-Yan production processes [18, 33, 37]. These latter processes are dominated by $q + \bar{q}$ initial states and jet production discussed in this manuscript arises primarily from $g + g$ (and $g + q(\bar{q})$ at larger E_T) processes.

Initial-state CNM effects in heavy ion collisions can be minimized by taking the ratio of jet cross section at two different radii $[d\sigma(R_1)/dE_T]/[d\sigma(R_2)/dE_T]$ [14]. Since the size R determines what fraction of the parton shower is reconstructed as a jet, it affects the jet cross section. In heavy ion reactions

²Two weeks after this manuscript was posted to the archive, the ATLAS Collaboration showed preliminary results on inclusive jet quenching in central Pb+Pb collisions at the Quark Matter 2011 conference. We include two data sets to give the reader a feel as to how the predictions presented here compare to the new data.

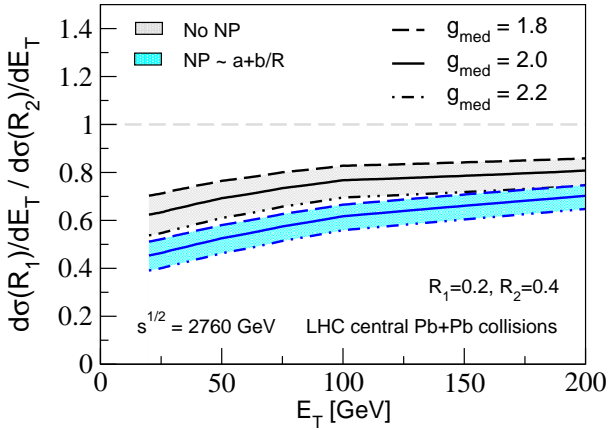


Figure 5: Ratio of the inclusive jet cross sections in central Pb+Pb collisions at LHC at $\sqrt{s_{NN}} = 2.76$ TeV for two different radii $R_1 = 0.2$ and $R_2 = 0.4$. The bands show results with different extrapolation of non-perturbative corrections to small radii. The lines show effect of different coupling strength between the jet and the medium.

the cone size dependence is amplified by the fact that medium-induced parton showers have a broad angular distribution in comparison to the ones in the vacuum [35]. This is shown in Fig. 5 for $R_1 = 0.2$, $R_2 = 0.4$ and the dashed, solid, and dot-dashed lines correspond to three different $g_{\text{med}} = 1.8, 2, 2.2$. As the radius varies, specific non-perturbative effects, unfortunately, become more important. Typically, they are expressed as an average momentum shift [2, 38] and related to “splash-out” hadronization effects and “splash-in” initial-state radiation/background contribution: $\langle \delta p_T \rangle = A/R + BR^2$. The physical effect of a momentum shift is to alter the measured cross section and this change can be isolated in a multiplicative factor [9]. Since background effects are the dominant uncertainty in jet physics with heavy ions, we will discuss them separately. With this motivation, we consider a hadronization-motivated extrapolation of the ATLAS parametrization of non-perturbative effects to small radii: $f_{NP} = a + b/R$. The application of this non-perturbative correction to the calculation of $[d\sigma(R_1 = 0.2)/dE_T]/[d\sigma(R_2 = 0.4)/dE_T]$ in central Pb+Pb collisions at the LHC is shown by the cyan band in Fig. 5, where we assume that for jet production at large E_T the “splash-out” hadronization effects in A+A collisions are the same as that in elementary p+p collisions with the understanding that the hadronization time for jets at high E_T is longer than the duration time of the QGP. Note that the non-perturbative effect can change significantly the cross section ratio relative to the $O(\alpha_s^3)$ parton level result for small R . It is, therefore, critical to constrain its magnitude as accurately as possible in the simpler p+p reactions. Moreover, higher order corrections may affect these ratios to some extent and a recent study has shown that in p+p collisions higher order correction may lower the jet cross section ratios considerably [38].

Preliminary RHIC results suggest that the jet size dependence of jet attenuation may have already been observed in Au+Au and Cu+Cu reactions at RHIC [15, 16, 17]. However, before we discuss di-jet production in heavy ion reactions, we

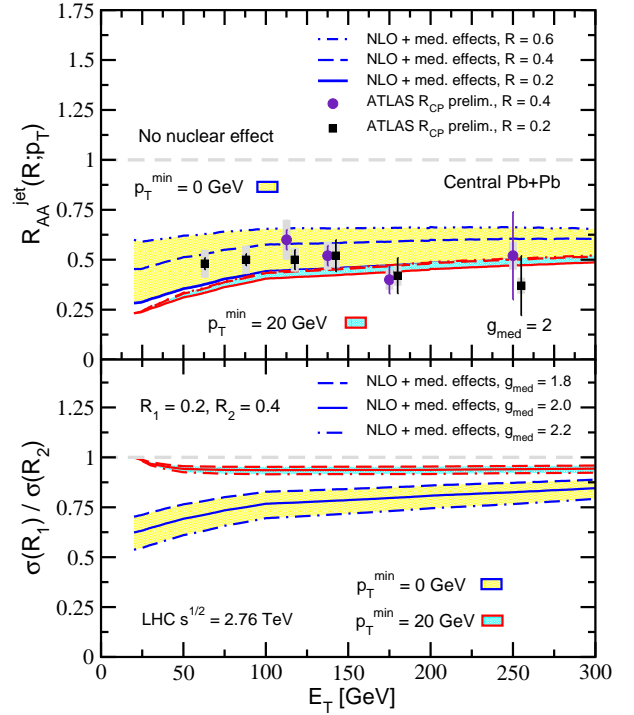


Figure 6: The effects of parton shower collisional energy loss or misinterpreting some of the jet’s energy as soft background on $R_{AA}^{1\text{-jet}}$ (top panel) and $\sigma(R_1)/\sigma(R_2)$ (bottom panel) are simulated with $p_T^{\text{min}} = 20$ GeV and represented by a cyan band. Results are contrasted to the $p_T^{\text{min}} = 0$ GeV case, represented by a yellow band, which is no collisional energy loss or unambiguous jet/background separation. Preliminary ATLAS R_{CP} data is shown for $R = 0.2, 0.4$.

comment on the difficulties related to the measurement of jet observables. In central Pb+Pb collisions at the LHC, for a typical jet size $R = 0.5$, on the order of 100 GeV of the jet energy is interpreted as QGP background and subtracted from the total reconstructed energy [20]. While a simple jet+uniform background model appears reasonable in heavy ion reactions, it is not based on first-principles theory. In what follows we demonstrate the consequences of misinterpreting less than 20 GeV of the jet energy redistributed by the QGP medium inside the jet as uncorrelated soft background. This is $< 20\%$ of the typical subtracted E_T and in our approach [13] can be simulated by choosing $p_T^{\text{min}} = 20$ GeV in Eq. (9). We denote the actual amount of energy by $\langle \delta E_T \rangle$ and emphasize that it depends on the jet radius R . More importantly, we recall that a recent calculation of the energy transmitted by a parton shower to the medium [27] $\Delta E(\text{shower} \rightarrow \text{QGP})$ found that for LHC conditions $\Delta E(\text{shower} \rightarrow \text{QGP}) \simeq 20$ GeV is well within reach, especially for a gluon-initiated shower. While the growth in the rate of collisional energy loss is due to the proliferation of medium-induced partons, the rate for each individual parton is calculated to $O(g_{\text{med}}^4)$. Of course, one should keep in mind that experimental observables are sensitive to the physics effects on the fraction of the in-medium parton shower that falls within the cone radius R . We first choose $p_T^{\text{min}} = 20$ GeV to simulate the collisional energy loss effects evaluated in [27] on the parton

shower for a very large radius $R \simeq 2$. We then vary R to obtain the collisional energy loss effect on the part of the parton shower that constitutes the jet. For example, for a 100 GeV gluon jet choosing $p_T^{\min} = 20$ GeV in Eq. (9) leads to $\langle \delta E_T \rangle \simeq 15$ GeV for $R = 0.5$ and to $\langle \delta E_T \rangle \simeq 5$ GeV for $R = 0.2$. The effect of collisional energy loss decreases quickly with the jet radius since the medium-induced parton shower has a characteristic large-angle [35] distribution and most of it is already outside of the jet cone for small R [13, 14, 18].

The result of our simulations is shown in Fig. 6 for $g_{\text{med}} = 2$, where the default choice $p_T^{\min} = 0$ GeV is illustrated by a yellow band and the choice $p_T^{\min} = 20$ GeV - by a cyan band. In the top panel, the clear dependence of $R_{AA}^{1\text{-jet}}$ on the jet size, exemplified by $R = 0.2, 0.4, 0.6$, practically disappears if a sizable fraction of the particles created by the medium-induced bremsstrahlung diffuse outside of the jet due to collisional processes or are subtracted as soft background. It can easily be seen that in this case and in the absence of strong R -dependent non-perturbative corrections $\sigma(R_1)/\sigma(R_2) \approx 1$. This is demonstrated in the bottom panel of Fig. 6 for three $g_{\text{med}} = 1.8, 2, 2.2$ and the result is very different in comparison to letting $p_T^{\min} = 0$ GeV. We do not include the non-perturbative correction in the bottom panel of Fig. 6 since it can result in noticeably different cross sections for significantly different R_1, R_2 and will distract from the difference between the simulations that only include radiative energy loss processes and the ones that include the effects of the collisional interactions of the parton shower. We conclude that the ambiguity in the jet/background separation and the possibility that some of the parton shower energy can diffuse away from the jet axis at angles greater than R through collisional processes [27] in heavy ion reactions can significantly affect the experimental jet cross sections.

3.2. Quenching of di-jets and their E_T asymmetry

We now present our results for the modification of di-jet production in central Pb+Pb collisions at $\sqrt{s_{NN}} = 2.76$ TeV. The cross section is evaluated using Eq. (10). First, we give a 3D representation for the suppression ratio $R_{AA}^{2\text{-jet}}$ of the di-jet cross section at $O(\alpha_s^3)$ in Pb+Pb collisions relative to the theoretically computed p+p baseline in Fig. 7. In this example we use jets with identical cone size $R = 0.2$, a coupling strength between the jets and the medium $g_{\text{med}} = 2$, and no transverse energy cut. The suppression involving both cold nuclear matter effects and final-state quenching effects in the QGP is the largest along the diagonal $E_{T1} = E_{T2}$. In the regime $E_{T1} \gg E_{T2}$ or $E_{T1} \ll E_{T2}$ there is a striking enhancement that can reach values much larger than 4 (the maximum value shown on the z axis in Fig. 7). Such enhancement was first identified theoretically on the example of Z^0 tagged jets [18] and is easy to understand. The final-state inelastic interactions of jets produced in heavy ion collisions redistribute them to smaller transverse energies and these jets fill in a region of phase space where the cross section is steeply falling, see Fig. 2. The second important observation is how broad the region of approximately constant $R_{AA}^{2\text{-jet}}$ in the (E_{T1}, E_{T2}) plane is before it hits the strong di-jet enhancement. This behavior limits the features in the heavy

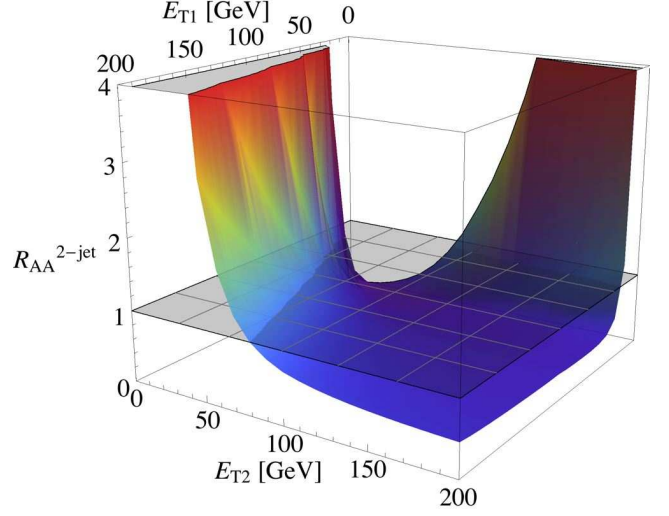


Figure 7: $O(\alpha_s^3)$ calculation of the di-jet cross section suppression ratio $R_{AA}^{2\text{-jet}}$ versus E_{T1} and E_{T2} in $\sqrt{s_{NN}} = 2.76$ TeV central Pb+Pb collisions at the LHC. Our result is for $R_1 = R_2 = 0.2$ and includes cold nuclear matter effects.

ion A_J enhancement that can be attributed to the physics of jet quenching.

Next, the di-jet asymmetry is computed using Eq. (6) and compared to recent experimental results published by ATLAS [19] and CMS [20] in Fig. 8 and Fig. 9. The ATLAS and CMS experiments apply different transverse energy cuts for their leading and subleading jets: $(E_{T1} > 100$ GeV, $E_{T1} > E_{T2} > 25$ GeV) and $(E_{T1} > 120$ GeV, $E_{T1} > E_{T2} > 50$ GeV), respectively. Two different calculations are performed and shown in the top and bottom panels of Figs. 8 and 9. In all cases the baseline p+p asymmetry at $\sqrt{s} = 2.76$ TeV is shown by a solid black line. Note that we present the normalized asymmetry result $(1/\sigma)d\sigma/dA_J$.

Fig. 8 shows the sensitivity of the di-jet asymmetry to the coupling strength g_{med} of the jets to the QGP medium. We use one jet size $R = 0.4$ (we will vary R later). This $p_T^{\min} = 0$ GeV case is represented by green curves. Qualitatively, we find a broadening of the di-jet asymmetry distribution but the dependence of this broadening to the variation of $g_{\text{med}} = 1.8, 2, 2.2$ is quite modest. Quantitatively, approximately 1/3 to 1/2 of the extra broadening that experiments attribute to jet interactions in matter can be described. Next, we consider collisional interactions of the parton shower or an ambiguity in the separation of the jets from the background in central Pb+Pb reactions at the LHC. This is represented and modeled by $p_T^{\min} = 20$ GeV and shown by red lines in Fig. 8. In this case, a significantly larger broadening is observed. However, only part of it is due to radiative jet quenching processes. The remainder may be due to removing the soft particles originating from the medium-induced parton shower inside the jet as uncorrelated soft background. In this sense, our result is similar to the argument presented in [25] that background fluctuations can generate much of the asymmetry observed by ATLAS and CMS. Alternatively, there is the possibility that this energy is dissipated outside the cone through collisional processes [27], something that we will in-

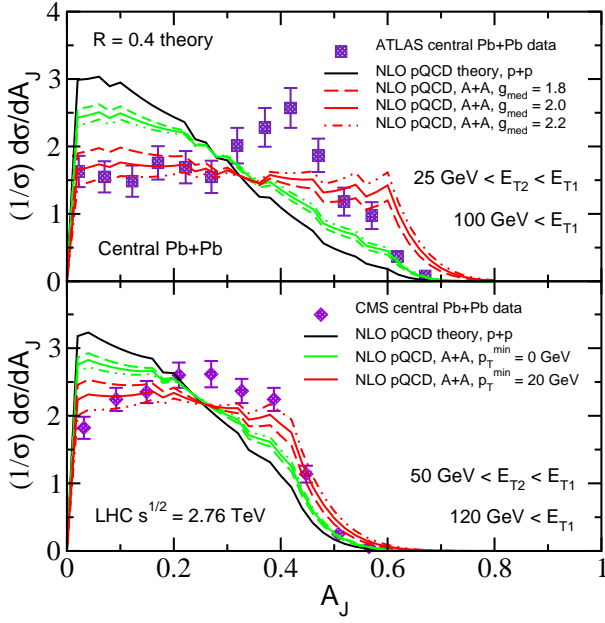


Figure 8: Di-jet asymmetry distributions for different coupling strength in central Pb+Pb collisions at $\sqrt{s} = 2.76$ TeV compared to data. The top panel is for leading jets of $E_{T1} > 100$ GeV, subleading jets of $E_{T2} > 25$ GeV (ATLAS [19], $R = 0.4$). The bottom panel is for leading jets of $E_{T1} > 120$ GeV, subleading jet of $E_{T2} > 50$ GeV (CMS [20], $R = 0.5$). Black lines are the results for p+p collisions under pQCD theory. Green lines assume perfect jet/background separation and are denoted $p_T^{\min} = 0$ GeV. Red lines, denoted $p_T^{\min} = 20$ GeV, show the consequences of the ambiguity in the jet/background separation or the diffusion of the in-medium parton shower energy away from the jet axis due to collisional processes.

investigate further in the future. This scenario is also modeled by $p_T^{\min} = 20$ GeV and in this case we have made quantitative connection to theoretical simulations [27]. We finally point out that even if all the energy associated with the medium-induced parton shower is removed, the resulting A_J distribution is flat. Specifically, a peak in this distribution at finite $A_J = 0.3 - 0.4$ is not compatible with realistic jet quenching calculations³. This is easy to be understood from the $O(\alpha_s^3)$ results presented here. The interested reader can analyze Fig. 7 and see that the flat A_J distribution is related to the very broad approximately constant $R_{AA}^{2\text{-jet}}$.

Fig. 9 shows the dependence of the di-jet asymmetry on the jet radius R and the the momentum cut p_T^{\min} with a fixed coupling strength $g_{\text{med}} = 2$. Note that for $p_T^{\min} = 0$ GeV there is a significant dependence on the jet size. For $p_T^{\min} = 20$ GeV, the dependence on the radius is practically eliminated. This observation is compatible with the comment by the ATLAS Collaboration [19] that their asymmetry measurement has little sensitivity to the choice of R over a wide range of cone sizes $R = 0.2 - 0.6$. It once again stresses the importance of considering the interaction between the full parton shower and the QGP

³At the recent QM2011 conference, after the results presented in this manuscript were posted to the archive, the ATLAS Collaboration presented a re-analysis of their A_J measurement with improved background subtraction. The peak at $A_J \approx 0.4$ is no longer present and the new distribution is consistent with flat up to the kinematic bound.

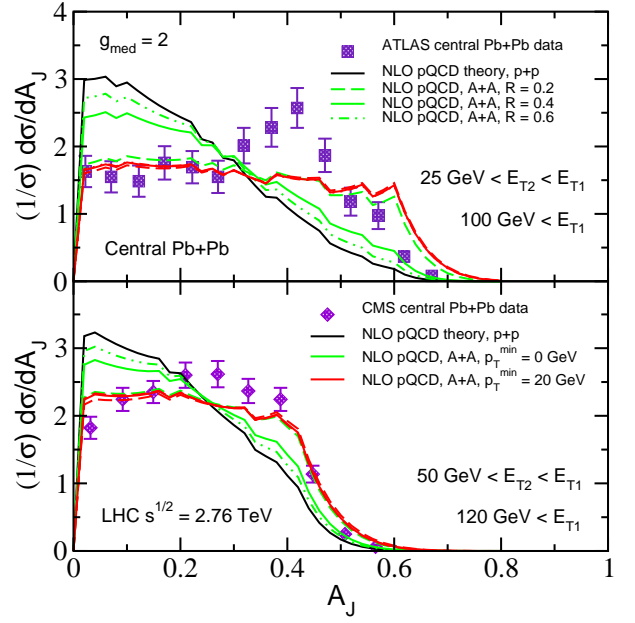


Figure 9: Same as Fig 8, but for a fixed jet-medium interaction strength $g_{\text{med}} = 2$. Dot-dashed, solid, and dashed lines correspond to $R = 0.6, 0.4, 0.2$ respectively. Note that if some of the subtracted “background” is in fact related to the medium-induced parton shower or energy diffuses away from the jet axis due to collisional processes, the enhanced asymmetry becomes radius-independent.

beyond the medium-induced parton splitting processes [27] and/or the ambiguity in the experimental jet/background separation [4].

4. Summary and Conclusions

Jet production and modification in high-energy nucleus-nucleus collisions have been proposed as new ways to unravel the properties of the hot and dense QCD medium and to elucidate the mechanisms of in-medium parton shower formation [13, 14, 18]. Measurements of jets in heavy ion collisions have now become available [15, 16, 17]. With this in mind, in this Letter we presented first $O(\alpha_s^3)$, $O(\alpha_s^2 \alpha_s^{\text{rad}})$ results for the single and double inclusive jets production rates in p+p and central Pb+Pb collisions at the LHC at center-of-mass energies per nucleon-nucleon pair $\sqrt{s_{NN}} = 7$ TeV and 2.76 TeV, respectively. We placed emphasis on the good agreement between the perturbative QCD theory and the experimental measurements in p+p collisions. The importance of reliable $O(\alpha_s^3)$ calculation cannot be under emphasized, since for tagged jets and di-jets an inaccurate description of the p+p baseline at LO can produce even qualitatively incorrect jet quenching predictions [18].

We first addressed the suppression of inclusive jet production in central Pb+Pb collisions at the LHC and found that it is dominated by final-state inelastic parton interactions in the QGP. Cold nuclear matter effects [31, 32, 33], even though larger than those for inclusive Z^0 production [37], still do not contribute significantly to the attenuation of jets for $R \leq 0.4$. On the other hand, there is a clear dependence of $R_{AA}^{1\text{-jet}}$ on the

coupling strength between the jet and the medium g_{med} . We found that for small radii the suppression of jets matches onto the suppression of leading particles [14], here represented by the ALICE charged hadron measurement. Cold nuclear matter effects can be practically eliminated by taking the ratio of the cross sections at two different jet sizes $\sigma(R_1)/\sigma(R_2)$, but in this case there is a sensitivity to the non-perturbative hadronization effects. We used an extrapolation of the ATLAS parametrization of non-perturbative effects [5] to show that for small radii $R \sim 0.2$ they can alter the cross section ratios by as much as 50%. It is important in the future to extend the experimental measurements to lower E_T and better constrain the magnitude of the non-perturbative effects.

Theoretically a clean calculation that focuses on the medium modification of jets is easy to perform. Experimentally, the situation is much more complicated in heavy ion reactions where there is an enormous soft background that may contribute ~ 100 GeV to the E_T of an $R = 0.5$ jet at the LHC. The problem of this background separation is both technical and conceptual since there is no unified first-principle understanding of heavy ion dynamics at all momentum scales. In our calculation we investigated the experimental consequences of this ambiguity by simulating a subtraction of a radius-dependent $\langle \delta E_T \rangle$ from the medium-induced parton shower as a part of the soft uncorrelated background. Such amount of energy $\langle \delta E_T \rangle$ may also easily be transferred from a 100 GeV shower to the medium through collisional processes. The first possibility *emulates* energy loss. The second possibility *is* the collisional energy loss of the parton shower that falls inside the jet cone radius R . We used the calculation in Ref [27] to constrain its magnitude. We found that such subtraction wipes out the jet size dependence of the quenching observables.

We also presented the first calculation of the di-jet modification $R_{AA}^{2\text{-jet}}$ in heavy ion reaction and found that it is characterized by a broad suppression region near $E_{T1} = E_{T2}$ and strong enhancement for $E_{T1} \gg E_{T2}$ or $E_{T1} \ll E_{T2}$. The resulting $O(\alpha_s^3)$ di-jet cross section was used to evaluate the di-jet asymmetry A_J . Assuming perfect jet/background separation we found that less than 1/2 of the broadening can be accounted for the radiative jet quenching calculation. We found little sensitivity of the A_J observable to the strength of the coupling between the jet and the medium and practically no dependence on the non-perturbative hadronization corrections. On the other hand, we found a clear dependence on the jet cone size R that can be correlated to the suppression of inclusive jets. If part of the energy of the medium-induced parton shower is additionally lost either through subtraction as soft background or through collisional processes, significantly larger enhancement in asymmetric jet production can be obtained for radii of moderate size $R = 0.4 - 0.5$. For small radii, such as $R = 0.2$, practically all of the asymmetry is due to radiative processes. Finally, the full calculation has no sensitivity to the choice of the cone radius R .

The ambiguity of jet/background separation and the diffusion of the in-medium parton shower energy through collisional processes [27] may play an important role in the generation of A_J . Recovery of the lost energy at large angles outside of the jet

cone [20] would tend to favor the latter scenario. We are currently looking for new observables [40] that have reduced sensitivity to QGP background fluctuations but retained clear dependence on the amount of collisional energy loss of the parton shower. We finally point out that a statistical peak in the asymmetry distribution at finite $A_J = 0.4 - 0.5$ is likely not related to the physics of jet quenching.

To summarize, significant experimental progress in jet physics in heavy ion collisions has been made to date. However, taken at face value, the PHENIX and STAR preliminary results in Au+Au and Cu+Cu collisions at RHIC [15, 17] and the ATLAS and CMS jet results in Pb+Pb collisions at the LHC [19, 20] do not allow, at present, to construct a consistent picture of jet modification in heavy ion reactions. Specifically, the pronounced dependence of the inclusive jet R_{AA} on the cone radius R at RHIC is inconsistent with argued independence of the di-jet asymmetry A_J on R . Such independence can easily arise from the inherent ambiguity in the separation of the jet from the enormous soft background in heavy ion reactions. It can also be related to the diffusion of a part of the in-medium parton shower energy away from the jet axis due to collisional processes. The ATLAS and CMS di-jet measurements have played an important role in emphasizing the importance of jet studies in heavy ion reactions at the LHC. However, a more comprehensive suite of measurements of inclusive jet and di-jet modification and further developments in theory are necessary to find a consistent picture of jet production and modification in dense QCD matter.

Acknowledgments: We thank D. Soper for helpful discussion. This research is supported by the US Department of Energy, Office of Science, under Contract No. DE-AC52-06NA25396 and in part by the LDRD program at LANL, and by the Ministry of Education of China with the Program NCET-09-0411, by Natural Science Foundation of China with Project No. 11075062, NSF of Hubei with Project No. 2010CDA075 and CCNU with Project No. CCNU09A02001.

References

- [1] J. M. Campbell, J. W. Huston and W. J. Stirling, Rept. Prog. Phys. **70**, 89 (2007); S. D. Ellis *et al.* Prog. Part. Nucl. Phys. **60**, 484 (2008).
- [2] F. I. Olness, D. E. Soper, Phys. Rev. **D81**, 035018 (2010).
- [3] M. Dasgupta, L. Magnea, G. Salam, JHEP **0802**, 055 (2008).
- [4] M. Cacciari, J. Rojo, G. P. Salam, G. Soyez, JHEP **0812**, 032 (2008).
- [5] G. Aad *et al.* [ATLAS Collaboration], Eur. Phys. J. **C71**, 1512 (2011).
- [6] V. Khachatryan *et al.* [CMS Collaboration], Phys. Lett. **B698**, 196-218 (2011).
- [7] M. Gyulassy and X. N. Wang, Nucl. Phys. B **420**, (1994) 583; R. Baier, Y. L. Dokshitzer, A. H. Mueller, S. Peigne and D. Schiff, Nucl. Phys. B **484**, (1997) 265; B. G. Zakharov, JETP Lett. **65**, (1997) 615; U. A. Wiedemann, Nucl. Phys. B **588**, (2000) 303; M. Gyulassy, P. Levai and I. Vitev, Nucl. Phys. B **594**, (2001) 371; X. N. Wang and X. F. Guo, Nucl. Phys. A **696**, (2001) 788.
- [8] A. Majumder and M. Van Leeuwen, Prog. Part. Nucl. Phys. A **66** (2011) 41.
- [9] I. Vitev, Phys. Lett. **B639**, 38-45 (2006).
- [10] A. Adare *et al.* [PHENIX Collaboration], Phys. Rev. Lett. **101**, 162301 (2008).
- [11] B. I. Abelev *et al.* [STAR Collaboration], Phys. Rev. **C80**, 044905 (2009).

- [12] K. Aamodt *et al.* [ALICE Collaboration], Phys. Lett. B **696**, 30 (2011)
- [13] I. Vitev, S. Wicks and B. W. Zhang, JHEP **0811**, 093 (2008).
- [14] I. Vitev and B. W. Zhang, Phys. Rev. Lett. **104**, 132001 (2010) [arXiv:0910.1090 [hep-ph]].
- [15] S. Salur, J. Phys. Conf. Ser. **230**, 012008 (2010).
- [16] J. Jia [PHENIX Collaboration], Nucl. Phys. A **855**, 92-100 (2011).
- [17] M. Ploskon [STAR Collaboration], Nucl. Phys. A **830**, 255C-258C (2009).
- [18] R. B. Neufeld, I. Vitev and B. W. Zhang, Phys. Rev. C **83**, 034902 (2011) [arXiv:1006.2389 [hep-ph]].
- [19] G. Aad *et al.* [Atlas Collaboration], Phys. Rev. Lett. **105**, 252303 (2010).
- [20] S. Chatrchyan *et al.* [CMS Collaboration], [arXiv:1102.1957 [nucl-ex]].
- [21] J. Casalderrey-Solana, J. G. Milhano, U. A. Wiedemann, J. Phys. G **G38**, 035006 (2011).
- [22] G. -Y. Qin, B. Muller, [arXiv:1012.5280 [hep-ph]].
- [23] I. P. Lokhtin, A. V. Belyaev, A. M. Snigirev, [arXiv:1103.1853 [hep-ph]].
- [24] C. Young, B. Schenke, S. Jeon, C. Gale, [arXiv:1103.5769 [nucl-th]].
- [25] M. Cacciari, G. P. Salam, G. Soyez, arXiv:1101.2878 [hep-ph].
- [26] I. Vitev, Prog. Theor. Phys. Suppl. **187**, 68 (2011) [arXiv:1010.5803 [hep-ph]].
- [27] R. B. Neufeld and I. Vitev, arXiv:1105.2067 [hep-ph].
- [28] J. F. Owens, Rev. Mod. Phys. **59** (1987) 465.
- [29] S. D. Ellis, Z. Kunszt and D. E. Soper, Phys. Rev. Lett. **64** (1990) 2121; Z. Kunszt and D. E. Soper, Phys. Rev. D **46** (1992) 192.
- [30] G. Ovanessian, I. Vitev, [arXiv:1103.1074 [hep-ph]].
- [31] I. Vitev, B. W. Zhang, Phys. Lett. B **669**, 337 (2008); R. Sharma, I. Vitev, B. Zhang, Phys. Rev. C **80**, 054902 (2009).
- [32] I. Vitev, Phys. Rev. C **75**, 064906 (2007).
- [33] R. B. Neufeld, I. Vitev and B. W. Zhang, arXiv:1010.3708 [hep-ph].
- [34] K. Aamodt *et al.* [The ALICE Collaboration], Phys. Rev. Lett. **105**, 252301 (2010).
- [35] M. Gyulassy, P. Levai and I. Vitev, Phys. Rev. Lett. **85**, 5535 (2000); I. Vitev, Phys. Rev. C **75**, 064906 (2007).
- [36] P. Steinberg, QM2011 talk; B. Cole, QM2011 talk
- [37] S. Chatrchyan *et al.* [CMS Collaboration], [arXiv:1102.5435 [nucl-ex]].
- [38] G. Soyez, Phys. Lett. B **698**, 59-62 (2011).
- [39] J. Pumplin, D. R. Stump, J. Huston, H. L. Lai, P. M. Nadolsky, W. K. Tung, JHEP **0207**, 012 (2002). [arXiv:hep-ph/0201195 [hep-ph]].
- [40] R. B. Neufeld and I. Vitev, arXiv:1202.5556 [hep-ph].